

Research Article

Role of Contrast-Enhanced Ultrasound in the Evaluation of Vascularization of Intrahepatic Cholangiocarcinoma

Giancarlo Gismondo Velardi^{*}, Matilde Lico¹, Rosario Maccarone¹, Marcello Ferrari¹, Angela Teti¹, Letterio Militano¹, Giuseppe Casuscelli¹, Ilaria V. Trecroci¹, Giuseppe Loria², Saverio Loria³, Sveva Loria⁴, Michela Basile¹, Francesca Frosina⁵, Francesco Loria¹

¹Department of Radiology, Jazzolino Hospital, ASP Vibo Valentia, Italy

²Department of Radiology, Giovanni Paolo II Hospital, ASP Catanzaro, Italy

³Faculty of Medicine, UMG Catanzaro, Italy

⁴International University Unicamillus, Italy

⁵General Medicine, ASP Reggio Calabria, Italy

Abstract

Aim: The aim of this report is to evaluate the role of Contrast-Enhanced Ultrasound (CEUS) in the vascularization of ICC, with regards to the start of contrast-enhancement time in the lesion during the arterial phase.

Methods: 52 patients who presented nodular hepatic lesions suspected for intrahepatic cholangiocarcinoma were examined by CEUS and enrolled in the study.

Results: We observed 3 Contrast-Enhancement (CE) pattern in the arterial phase in 52 nodules considered as ICC: peripheral rim-like enhancement (36/52), incomplete heterogeneous fill-in (8/52), complete homogeneous fill-in (6/52) and 2 cases of intraductal ICC with peripheral rim-enhancement. The arterial enhancement is always characterized (100%) by an early wash-in (in a time between 11 and 22 s) and wash-out (22-35 s).

Conclusion: CEUS is a method capable of documenting with very reliable accuracy the intralesional vascularization of intrahepatic cholangiocarcinoma. However, CEUS also presents some limitations, mainly in relation to the location of lesions.

Keywords: Intrahepatic cholangiocarcinoma; Liver; Contrast-enhanced ultrasound; Early diagnosis

Introduction

Intrahepatic Cholangiocarcinoma (ICC) arises from the epithelium of second order branches of the biliary system, mostly after chronic inflammation of the intrahepatic biliary ducts such as primary sclerosing cholangitis. After Hepatocarcinoma (HCC), ICC is the second malignant hepatic tumor, with an incidence of about 1-2 per 100.000 [1].

Due to the delayed diagnosis, this tumor has poor prognosis: only 15% of tumors is resectable at diagnosis, with median survival of less than 3 years. To achieve the best clinical outcome, early detection is mandatory for useful treatment [1].

B-Mode ultrasound in association with Color-Doppler is the first-line imaging method in the detection of Focal Liver Lesions (FLLs), but its specificity is limited [2]. The development of second-generation contrast agents and of modern dedicated

software has improved the diagnostic value of US in detection and characterization of focal liver lesions, allowing the evaluation of intralesional vascularization in real-time during all the contrast phases [2,3]. The aim of this work is to evaluate the vascularization of ICC during arterial phase considering the precocity of the time of wash-in and wash-out.

Methods

Between December 2019 and January 2023, 370 patients, without underlying liver disease, affected by single FLL were examined: 160 patients with HCC, 2 metastasis, 50 atypical hemangiomas, 15 atypical adenomas, 6 focal abscesses, 15 atypical focal nodular hyperplasia. 52/370 had ultrasound signs suspicious for intrahepatic cholangiocarcinoma, such as irregular margins, parenchymal retraction with associated homogeneous or inhomogeneous findings, district biliary dilatation. The patients were included in this retrospective study: they were 20 females and 32 males with an average age of 67 years and Body Mass Index (BMI) of about 26. In 28 patients, the lesion was discovered incidentally during B-Mode examination; in 24 it was discovered due to clinical manifestations as abdominal discomfort, abdominal pain, nausea, weight-loss, weakness, rapid decline in performance status.

In B-mode examination, 8 nodules (15.4%) were slightly hyperechoic (of these, 4 with halo sign), 22 (42.3%) hypoechoic (of these, 4 with halo sign), 8 (15.4%) isoechoic and 14 (26.9%) with heterogeneous appearance. Margins were defined in 57.6% (30/52) of the cases, poorly defined in 43.4% (22/52). 12 nodules (23.1%)

Citation: Gismondo Velardi G, Lico M, Maccarone R, Ferrari M, Teti A, Militano L, et al. Role of Contrast-Enhanced Ultrasound in the Evaluation of Vascularization of Intrahepatic Cholangiocarcinoma. *CMJ Oncol.* 2024; 1(1): 1001.

Copyright: © 2024 Giancarlo Gismondo Velardi

Publisher Name: MedClinics Journals

Received: May 02, 2024; **Accepted:** May 27, 2024; **Published:** May 29, 2024

***Corresponding author:** Giancarlo Gismondo Velardi, Department of Radiology, Jazzolino Hospital, ASP Vibo Valentia, Vibo Valentia, Italy E-mail: ggvs84@hotmail.com

sized ≤ 3 cm, and 40 (76.9%) more than 3 cm. These characteristics are summarized in Table 1. 16 lesions were located in the left lobe (in segment II/III), 20 were located medially in segment IV, 10 were located in the right segments (V, VI, VII, VIII), and 6 involved more than three segments (3 right and 3 left).

16 patients had elevated CA19-9 levels (average value of about 133 U/ml); elevated Alpha-Fetoprotein (AFP) (110 ng/ml) and Carcinoembryonic Antigen (CEA) (19 ng/ml) levels were detected in only one patient respectively.

In all patients the diagnosis was confirmed by surgery or biopsy.

The Ethical Board of the hospital approved this study.

Table 1: B-Mode appearance of ICC.

Echogenicity	N° (%)
Hypochoic	22 (42.3%)
Isochoic	8 (15.4%)
Slightly hyperechoic	8 (15.4%)
Heterogeneous	14 (26.9%)
Size	
<3 cm	12 (23.1%)
>3 cm	40 (76.9%)
Margins	
Defined	30 (57.6%)
Poorly defined	22 (43.4%)

CEUS

The examinations were performed with ESAOTE MY LAB 9 and ESAOTE X 90 equipment with a contrast specific mode at low mechanical index, with 3.5/1-8 MHz convex transducers. SonoVue (Bracco, Italy) is the contrast medium employed; it consists of micro bubbles of stabilized phospholipids containing Sulphur hexafluoride. An intravenous bolus injection of SonoVue at the dose of 2,4 ml was first administered, followed by a flush of 5 ml saline solution, using a 20-gauge catheter.

The liver was examined by B-Mode sonography in all patients before the contrast media injection to identify the most feasible scan plan for the study of the target lesion.

All lesions were studied in real-time up to approximately 5 minutes from the start of injection. All examinations were recorded on a digital support. No adverse reactions were observed in any patient.

Images analysis

Two radiologists, with more than 10-years' experience in CEUS of the liver, analyzed (separately and independently of the radiologist who performed the examinations), the registered examinations on digital support (DVD). Any data of patients was hidden to the readers.

During the review, we considered an extended arterial phase (0-35 seconds), portal phase (36-90 seconds) and late phase (>90 seconds). We extended the arterial phase to 35 seconds to evaluate the start of the wash-out phase.

To check the sensitivity, specificity, diagnostic accuracy and predictive positive value, of precocity of wash-in and wash-out of contrast medium into the lesions, we also evaluated these two phases during arterial phase in a control group of patients with HCC.

Diagnostic criteria

Based on the known semeiological findings in the literature, we considered as sign of ICC the presence of rim-like enhancement with incomplete fill-in during arterial phase and rapid wash-out during portal and late phase. Also, we considered as sign of ICC the presence of wash-in during the first arterial phase (0-22 seconds) and wash-out starting during the late arterial phase (22-35 seconds) in the lesion with homogeneous or inhomogeneous enhancement.

We analyzed in real time the lesion evaluating during arterial phase these findings: the start of vascularization within the lesion; distribution of vascularization within the lesion, central or peripheral; complete fill-in (homogeneous) or incomplete fill-in (inhomogeneous); start of the wash-out; size of the nodules (\leq of 3 cm and $>$ of 3 cm).

Also, we analyzed the time of wash-in and wash-out of HCC: in these lesions the wash-in started from 20 seconds and wash-out from 50 seconds.

Statistical analysis

Fisher's test was used to evaluate the diagnostic capabilities of CEUS in terms of sensitivity, specificity, diagnostic accuracy and positive predictive value.

These values were evaluated in comparison with semeiological data reported in the literature.

Results

During the arterial phase 36 nodules (69.2%) had peripheral distribution of vascularization (rim-like enhancement, Figure 1), 8 (15.3%) had incomplete fill-in with heterogeneous enhancement (Figure 2), 6 (11.5%) had complete fill-in with homogeneous enhancement (Figure 3) and 2 (3.8%) were intraductal ICC with peripheral distribution of vascularization. The 2 cases of ICC with intraductal development had sharp, defined margins with regular capsular enhancement, in contrast to the larger lesions that show rim-like enhancement with finely irregular, bumpy margins. All lesions appeared as hypo vascular in portal and late phase. These findings are summarized in Table 2.

The lesions with diameter >3 cm (40/52) showed: 20 (50%) peripheral rim-like enhancement, 10 (25%) incomplete inhomogeneous enhancement and 10 (25%) complete homogeneous enhancement. Lesions with diameter ≤ 3 cm (12/52): 10 (83.3%) presented homogeneous enhancement and 2 (16.7%) peripheral rim enhancement. These data are reported in Table 3.

During the arterial phase, the presence of intralesional vascularization was observed from 11 to 22 seconds to the start of injection. The wash-out phase started from 28 to 35 seconds. In 4 lesions, the wash-out appeared after 36s. The wash-in and wash-out time of CE during arterial phase of the lesions is reported in Table 4.

Wash-out of contrast-media was observed in the portal and late phase in all cases, with aspect of hypo-enhancement (100%). During portal phase, in 18/36 patient (34.6%) who presented the arterial peripheral rim-like enhancement, a persistence of this finding was observed.

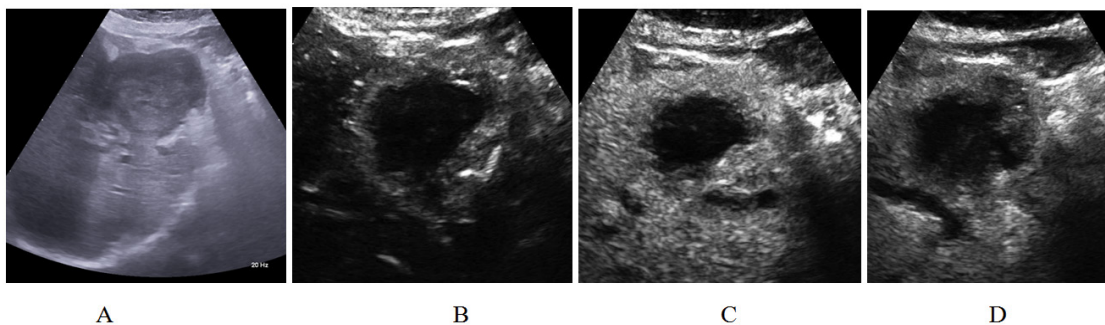


Figure 1: A) B-Mode ultrasound shows slightly hyperechoic, inhomogeneous eco structure nodule with slightly rough and irregular hypoechoic margins; B) Arterial phase (19 s): rim-like peripheral hyperenhancement with central minimal microcirculation; C) Portal phase (69 s): the nodule has peripheral wash-out with central hypo enhancement; D) Late phase: ICC nodule presents hypo enhancement.

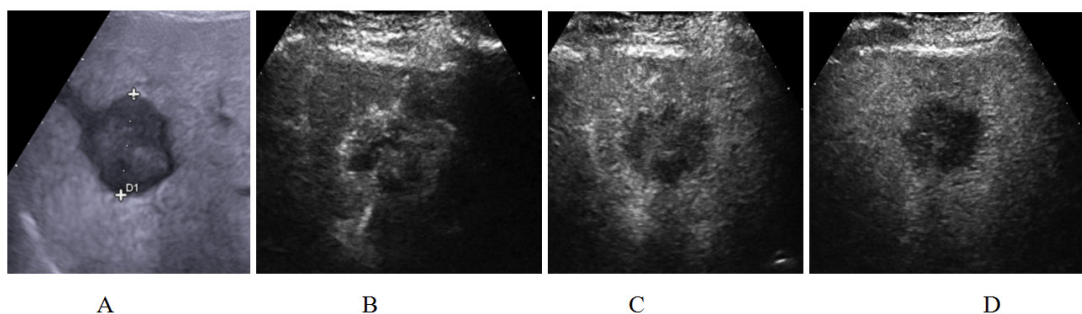


Figure 2: A) B-Mode ultrasound shows an unevenly hypoechoic nodule (caliper) and finely drafted irregular margins; B) During arterial phase, CE time started at 22 s and it is inhomogeneous; C) During portal phase (65 s): slight persistence of peripheral enhancement with intralesional wash-out is observed; D) Late phase shows hypo enhancement of the nodule.

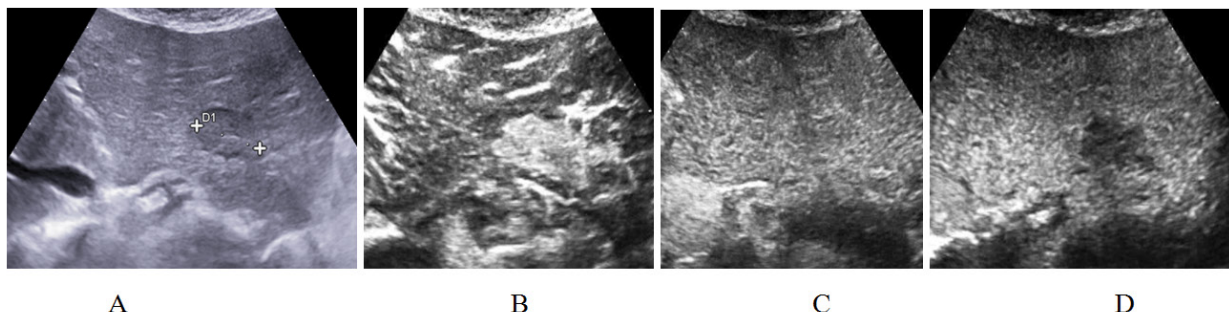


Figure 3: A) B-Mode ultrasound shows a homogenous iso-hypoechoic nodule with thin peripheral hypoechoic halo; B) During arterial phase the CE time of the lesion started after 17 s, with a complete and homogeneous hyperenhancement; During portal phase (C) and late phase (D), the nodule presents hypo enhancement.

2/52 lesion showing homogenous arterial enhancement (similarly to the other) with wash-out starting after 30 seconds. We erroneously classified these lesions as ICC. At pathological examinations after surgery, these lesions were classified as metastasis from rectal carcinoma.

The analysis of wash-in and wash-out of control group of patients with HCC revealed starting of wash-in time during arterial phase from 20 to 30 seconds and the start of wash out from 50-60 s.

These values sensitivity, specificity, diagnostic accuracy and positive predictive value of CEUS in diagnosis of ICC in our series are reported in Table 5.

Discussion

The development of dedicated software and the second-

generation contrast media implemented the role of CEUS in the detection and characterization of FLLs, due to the possibility to detect in real-time the vascularization. The second-generation US contrast medium (Sonovue), differently from contrast agents employed in CT and MR, has only endovascular distribution, without passage into the interstitial space [2]. In fact, CEUS can visualize more clearly the vascular patterns of the FLLs, giving additional information during all phases [4].

In the literature are reported 4 different patterns of CE of ICC in the arterial phase [5]: irregular peripheral hyper-enhancement, heterogeneous hyper-enhancement, homogeneous hyper-enhancement, heterogeneous hypo-enhancement. In the portal and late phases is reported the pattern of hypo vascularization in all cases.

Table 2: CEUS patterns.

Arterial phase	Nodules, n (%)
Peripheral rim enhancement	38 (73%)
Central enhancement	0 (0%)
Complete heterogeneous enhancement	8 (15.3%)
Complete homogeneous enhancement	6 (11.5%)
Portal phase	
Hypoenhancement	52 (100%)
Hyperenhancement	0 (0%)
Isoenhancement	0 (0%)
Late phase	
Hypoenhancement	52 (100%)
Hyperenhancement	0 (0%)
Isoenhancement	0 (0%)

Table 3: Arterial enhancement pattern in relation to the size of the nodules.

Arterial enhancement pattern	Nodules >3 cm, n (%)	Nodules ≤ 3 cm, n (%)
Rim enhancement	20 (50%)	2 (16,7%)
Central enhancement	0 (0%)	0 (0%)
Incomplete disomogeneous enhancement	10 (25%)	0 (0%)
Complete homogeneous enhancement	10 (25%)	10 (83,3%)

Table 4: Time of wash-in and wash-out during arterial phase.

Arterial wash-in	
Early (11-22 sec.)	52 (100%)
Late (>22 sec.)	0 (0%)
Arterial wash-out	
Early (28-35 sec.)	48 (92%)
Late (>35 sec.)	4 (8%)

Table 5: Sensitivity, specificity, diagnostic accuracy and positive predictive value of CEUS in ICC diagnosis in our series.

Total number of cases	Sensitivity	Specificity	Diagnostic accuracy	Positive predictive value (PPV)
52	100%	96%	98%	96%

In our series, we encountered 3 types of vascularization in the arterial phase: peripheral rim-like (73%), complete homogeneous (11.5%), or incomplete heterogeneous (15.3%). We didn't encounter during arterial phase the type of heterogeneous hypo-enhancement, because we considered the heterogeneous hypo-enhancement pattern as incomplete fill-in.

In all nodules (100%), we observed the start of vascularization in the early arterial phase, between 11 and 22 s, and the start of wash-out (92%) between 22-35 seconds, in 4 (8%) after 35 seconds. These findings, not reported in other reports, allow us for a correct diagnosis and may be considered as another signs of ICC. The control group of patients with HCC presenting the start of vascularization between 20-30 s and the start of wash-out after 60 s [3,6]. In fact, in no case of HCC was noted wash-out before 35 s.

The CE pattern reported in the literature during arterial phase can be influenced by the tumor size, in particular, ICC with dimension less than 5 cm generally shows a homogeneous enhancement (due to a minor fibrotic component), while if greater than 5 cm typically presents peripheral enhancement in the arterial phase and hypo vascularization in the portal and late phase [5].

In our series, the lesions with diameter >3 cm (40/52) showed: 20 (50%) peripheral rim enhancement, 10 (25%) incomplete and 10 (25%) complete enhancement. Lesions with diameter ≤ 3 cm (12/52): 10 (83.3%) presented homogeneous enhancement and 2

(16.7%) peripheral rim enhancement.

Jin et al. [7] retrospectively analyzed 64 ICC, divided into two groups depending on tumor size: 25 with dimensions <5 cm and 39 >5 cm. During the arterial phase, in the first group 31.3% had homogeneous hyperenhancement, 17.2% partial hyperenhancement and 51.6% peripheral enhancement; in the second group, 64% had homogeneous hyperenhancement, 8%, partial hyperenhancement, 28% peripheral enhancement. During the portal venous phase, in the first group 16% had an isoechoic aspect and 84% hypoechoic aspect; in the second group 7.7% had an isoechoic aspect and 92.3% hypo vascular aspect. In both groups, 100% of lesions were hypo vascular in the late phase [7].

Xu et al. [8] demonstrated that CEUS findings correlate areas of endo tumor hyper-enhancement, indicate an increase in tumor cell density. In this study, in the arterial phase, 59.4% had irregular peripheral hyperenhancement, 18.8% heterogeneous hyperenhancement, 9.4% homogeneous hyperenhancement, 12.5% homogeneous hypo enhancement, 28.1% had endolesional arterial vessels. In the portal phase, 96.9% had hypo enhancement, 3.1% iso enhancement. In the late phase, 100% of lesions have hypo vascular appearance [8].

The grade of microvascular density, arterial density, fibrous stroma, and necrosis may be responsible for the difference in the aforementioned enhancement patterns [9,10].

In our series, we found 36/52 cases of rim peripheral enhancement in arterial phase that, as suggested by Xu et al. [8], corresponds to increase in tumor cell density, while the central portion of the lesion with hypo vascular aspect corresponds to fibrous stroma.

Chen et al. [5] reported that the portal-venous peripheral enhancement rim (present in 66.7% of the lesions under evaluation in their retrospective study) can confirm the diagnosis of ICC as an expression of abundant cellularity in the peripheral part of the mass [5,11,12].

We emphasize the precocity of CE time during arterial phase: in all cases, the CE was ranged from 0-22 seconds and wash-out ranged from 22-35 seconds. We retain that this finding contributes to make a correct diagnosis of ICC, because it shows vascularization earlier than other focal liver lesions, particularly HCC usually presents start of wash-out after 60 seconds [3].

Based on these findings, in particular due to the evaluation of precocity of CE, in our series we reported sensitivity (100%), specificity (96%), diagnostic accuracy (98%) and positive predictive value (96%) of CEUS in ICC diagnosis. In the other series, were reported similar data regard sensitivity (78.8-91.3%), specificity (83.8-96.7%), diagnostic accuracy (84.3-96.5%), PPV (56.8-82.3%) [13-15].

We erroneously classified as ICC 2 colon-rectal metastasis because their CE time were similar as homogeneous ICC.

In the clinical practice, the use of CT is considered conclusive for the diagnosis in almost all patients, while MRI is only used in specific patients [16]. In the diagnosis of ICC, CT shows a sensitivity of 49-84,2%, specificity of 67.1-100%, diagnostic accuracy of 69-89.8%, PPV 92-100%, NPV 48-75%. MRI shows a sensitivity of 51-95.12%, specificity of 65.7-97.6%, diagnostic accuracy of 79-95.7%,

PPV 92%, NPV 76%. [17-22].

In addition, hepatospecific contrast agent (BOPTA and/or EOB) MRI may allow later sequences (cholangiography) to demonstrate hepatocyte alteration characterized by low signal intensity in the lesion, providing additional diagnostic evidence of malignancy [23].

CEUS is also well recognized for the ability to characterize liver lesions; its excellent diagnostic value was confirmed by several prospective studies, including the DEGUM study with over 1000 patients [24], the Romanian [25] and the French multicenter study [26].

CEUS showed the same accuracy of CT and MRI in the characterization of liver tumors [27,28]. Therefore, CEUS was included among the imaging techniques approved for the non-invasive diagnosis of HCC in the 2005 American Association of the Study of Liver Disease (AASLD) guidelines [29]. However, in a retrospective series of histologically confirmed cirrhosis patients with ICC, the Barcelona Clinic Liver Cancer (BCLC) team found out ten ICC patients with CEUS enhancement pattern similar to those considered diagnostic for HCC, or homogenous arterial enhancement followed by wash-out [30].

Based on these findings, CEUS was removed from diagnostic techniques for nodules in cirrhosis in the AASLD 2011 guidelines [31] and subsequently also from the European Association for the study of the Liver (EASL) guidelines [32,33]. However, this removal has raised many controversial arguments and has not been well accepted in Europe and Asia [34].

A clinical evaluation with tumor markers and biochemical tests are suitable to differentiate ICC from HCC. In fact, tumor markers represent an additional diagnostic tool for the diagnosis of ICC and for the differential diagnosis with HCC. In particular, CA19-9 shows increased values in patient with ICC [35], while Alpha-Fetoprotein (AFP) in HCC [36].

CEUS can be used in patients undergoing Radiofrequency Therapy (RFA) when the target is not clearly evident at baseline US. Also, it can be performed during treatment with RFA to detect the presence of micro vascularization within the lesion, making possible to evaluate the effectiveness [37,38].

The intrinsic limitations of CEUS are related to various patient characteristics such as obesity, patients' compliance, size, depth, and operator experience [39].

Another important limitation of CEUS consists on the examination performed on the single target. On the contrary, CT and MRI allow to evaluate the entire hepatic parenchyma.

When a differential diagnosis between benign and malignant lesion is not possible despite the use of different imaging methods, a strict follow up of the patient or a biopsy could be necessary, depending on the size of the lesion and clinical considerations [40].

Conclusion

CEUS is a not invasive, not stressful, rapid, economical and accurate tool for the diagnosis and management of ICC. The presence, during the arterial phase, of vascularization between 0 and 22 seconds, either with rim-like enhancement morphology, complete or incomplete fill-in, and the ultra-rapid wash-out (22-

36 s), allow a correct diagnosis of ICC, also plays a decisive role in differentiating ICC from HCC.

References

- Buettner S, van Vugt JL, IJzermans JN, Koerkamp BG. Intrahepatic cholangiocarcinoma: current perspectives. *Onco Targets Ther.* 2017;10:1131-42.
- Serra C, Righi S, Molo CD, Felicani C. Current role of contrast-enhanced ultrasound in the diagnosis of hepatocellular carcinoma. *J Hepatol Gastroint Dis.* 2015;1:102.
- Loria F, Loria G, Basile S, Crea G, Frosina L, Frosina F. Role of contrast-enhanced ultrasound in the evaluation of vascularization of hepatocellular carcinoma. *Hepatoma Res.* 2016;2:316-22.
- D'Onofrio M, Rozzanigo U, Masinielli BM, Caffarri S, Zogno A, Malagò R, et al. Hypoechoic focal liver lesions: characterization with contrast enhanced ultrasonography. *J Clin Ultrasound.* 2005;33(4):164-72.
- Chen T, Chang X, Lv K, Wang Y, Fu X, Tan L, et al. Contrast-enhancement ultrasound features of intrahepatic cholangiocarcinoma: a new perspective. *Sci Rep.* 2019;9(1):19363.
- European Association for the Study of the Liver. EASL clinical practice guidelines: Management of hepatocellular carcinoma. *J Hepatol.* 2018;69(1):182-236.
- Jin C, Zhang XY, Li JW, Li C, Peng W, Wen TF, et al. Impact of tumor size and cirrhotic background for differentiating HCC and ICC with CEUS: does it matter for patients undergoing hepatectomy? *Oncotarget.* 2017;8(48):83698-711.
- Xu HX, Chen LD, Liu LN, Zhang YF, Guo LH, Liu C. Contrast-enhanced ultrasound of intrahepatic cholangiocarcinoma: correlation with pathological examination. *Br J Radiol.* 2012;85:1029-37.
- Dietrich CF, Ignee A, Hocke M, Schreiber-Dietrich D, Greis C. Pitfalls and artefacts using contrast enhanced ultrasound. *Z Gastroenterol.* 2011;49(3):350-6.
- Yuan MX, Li R, Zhang XH, Tang CL, Guo YL, Guo DY, et al. Factors affecting the enhancement patterns of intrahepatic cholangiocarcinoma (ICC) on Contrast-enhancement ultrasound (CEUS) and their pathological correlations in patients with a single lesion. *Ultraschall Med.* 2016;37(6):609-18.
- Cerrito L, Ainora ME, Borriello R, Piccirilli G, Garcovich M, Riccardi L, et al. Contrast-enhanced imaging in the management of intrahepatic cholangiocarcinoma: State of art and future perspectives. *Cancers.* 2023;15(13):3393.
- Iavarone M, Piscaglia F, Vavassori S, Galassi M, Sangiovanni A, Venerandi L, et al. Contrast enhanced CT-scan to diagnose intrahepatic cholangiocarcinoma in patients with cirrhosis. *J Hepatol.* 2013;58(6):1188-93.
- Li R, Yuan MX, Ma KS, Li XW, Tang CL, Zhang XH, et al. Detailed analysis of temporal features on contrast enhanced ultrasound may help differentiate intrahepatic cholangiocarcinoma from hepatocellular carcinoma in cirrhosis. *PLoS One.* 2014;9(5):e98612.
- Vidili G, Arru M, Solinas G, Calvisi DF, Meloni P, Sauchella A, et al. Contrast-enhanced ultrasound liver imaging reporting and data system: lights and shadows in hepatocellular carcinoma and cholangiocellular carcinoma diagnosis. *World J Gastroenterol.* 2022;28(27):3488-502.
- Ainora ME, Cerrito L, Liguori A, Mignini I, Luca AD, Galasso L, et al. Multiparametric dynamic ultrasound approach for differential diagnosis of primary liver tumors. *Int J Mol Sci.* 2023;24(10):8548.
- Sun, D, Xu, Z, Cao S, Wu H, Lu M, Xu Q, et al. Imaging features based on CT and MRI for predicting prognosis of patients with intrahepatic cholangiocarcinoma: a single-center study and meta-analysis. *Cancer Imaging.* 2023;23(1):56.
- Li J, Yu Y, He Q. The auxiliary diagnosis and imaging characteristics of MRI combined with CT in patients with cholangiocarcinoma. *J Oncol.* 2021;2021:2790958.
- Lee SW, Kim HJ, Park JH, Park DI, Cho YK, Sohn CI, et al. Clinical usefulness of 18F-FDG PET-CT for patients with gallbladder cancer and cholangiocarcinoma. *J Gastroenterol.* 2010;45(5):560-6.
- Nishioka E, Tsurusaki M, Kozuki R, Im SW, Kono A, Kitajima K, et al. Comparison of conventional imaging and 18f-fluorodeoxyglucose positron emission tomography/

- computed tomography in the diagnostic accuracy of staging in patients with intrahepatic cholangiocarcinoma. *Diagnostics (Basel)*. 2022;12(11):2889.
20. Ke C, Yang T, Huang G, Gu C. Investigation of the accuracy of magnetic resonance cholangiography and multi-slice spiral computed tomography in the diagnosis of cholangiocarcinoma. *J Gastrointest Oncol*. 2023;14(3):1496-503.
 21. Kim YY, Yeom SK, Shin H, Choi SH, Rhee H, Park JH, et al. Clinical staging of mass-forming intrahepatic cholangiocarcinoma: computed tomography versus magnetic resonance imaging. *Hepatol Commun*. 2021;5(12):2009-18.
 22. Petrowsky H, Wildbrett P, Husarik DB, Hany TF, Tam S, Jochum W, et al. Impact of integrated positron emission tomography and computed tomography on staging and management of gallbladder cancer and cholangiocarcinoma. *J Hepatol*. 2006;45(1):43-50.
 23. Frydrychowicz A, Lubner MG, Brown JJ, Merkle EM, Nagle SK, Rofsky NM, et al. Hepatobiliary MR imaging with gadolinium-based contrast agents. *J Magn Reson Imaging*. 2012;35(3):492-511.
 24. Strobel D, Seitz K, Blank W, Schuler A, Dietrich C, von Herbay A, et al. Contrast-enhanced ultrasound for the characterization of focal liver lesions diagnostic accuracy in clinical practice (DEGUM multicentre trial). *Ultraschall Med*. 2008;29(5):499-505.
 25. Sporea I, Badea R, Martie A, Dumitru E, Ioanițescu S, Șirli R, et al. Contrast Enhanced Ultrasound for the evaluation of focal liver lesions in daily practice. A multicentre study. *Med Ultrason*. 2012;14(2):95-100.
 26. Tranquart F, Le Gouge A, Correas JM, Marcus VL, Manzoni P, Vilgrain V, et al. Role of contrast-enhanced ultrasound in the blinded assessment of focal liver lesions in comparison with MDCT and CEMRI: Results from a multicentre clinical trial. *Eur J Cancer Supplements*. 2008;6(11):9-15.
 27. Dietrich CF, Kratzer W, Strobel D, Danse E, Fessl R, Bunk A, et al. Assessment of metastatic liver disease in patients with primary extrahepatic tumors by contrast-enhanced sonography versus TC and MRI. *World J Gastroenterol*. 2006;12(11):1699-705.
 28. Sangiovanni A, Manini MA, Iavarone M, Romeo R, Forzenigo LV, Fraquelli M, et al. The diagnostic and economic impact of contrast imaging techniques in the diagnosis of small hepatocellular carcinoma in cirrhosis. *Gut*. 2010;59(5):638-44.
 29. Bruix J, Sherman M. Management of hepatocellular carcinoma. *Hepatology*. 2005;42(5):1208-36.
 30. Vilana R, Forner A, Bianchi L, García-Criado A, Rimola J, de Lope CR, et al. Intrahepatic peripheral cholangiocarcinoma in cirrhosis patients may display a vascular pattern similar to hepatocellular carcinoma on contrast-enhanced ultrasound. *Hepatology*. 2010;51(6):2020-9.
 31. Bruix J, Sherman M. Management of hepatocellular carcinoma: an update. *Hepatology*. 2011;53(3):1020-2.
 32. Galassi M, Iavarone M, Rossi S, Bota S, Vavassori S, Rosa L, et al. Patterns of appearance and risk of misdiagnosis of intrahepatic cholangiocarcinoma in cirrhotic at contrast enhanced ultrasound. *Liver Int*. 2013;33(5):771-9.
 33. European Association for the Study of the Liver. EASL-EORTC Clinical practice guidelines management of hepatocellular carcinoma. *J Hepatol*. 2012;56(4):908-43.
 34. Barreiros AP, Piscaglia F, Dietrich CF. Contrast enhanced ultrasound for the diagnosis of hepatocellular carcinoma (HCC): comments on AASLD guidelines. *J Hepatol*. 2012;57(4):930-2.
 35. He C, Zhang Y, Song Y, Wang J, Xing K, Lin X, et al. Preoperative CEA levels are supplementary to CA19-9 levels in predicting prognosis in patients with resectable intrahepatic cholangiocarcinoma. *J Cancer*. 2018;9(17):3117-28.
 36. Zong J, Fan Z, Zhang Y. Serum tumor markers for early diagnosis of primary hepatocellular carcinoma. *J Hepatocell Carcinoma*. 2020;7:413-22.
 37. Giorgio A, Gatti P, Montesarchio L, Santoro B, Dell'Olio A, Crucinio N, et al. Intrahepatic cholangiocarcinoma and thermal ablation: Long-term results of an Italian retrospective multicenter study. *J Clin Transl Hepatol*. 2019;7(4):287-92.
 38. Kim YS, Lim HK, Rhim H, Lee MW, Choi D, Lee WJ, et al. Ten-year outcomes of percutaneous radiofrequency ablation as first-line therapy of early hepatocellular carcinoma: analysis of prognostic factors. *J Hepatol*. 2013;58(1):89-97.
 39. Loria F, Loria G, Crea G, et al. Vascolarizzazione dell'epatocarcinoma: ruolo della CEUS e della TC multifasica [In italian: Vascularization of hepatocarcinoma: role of the CEUS and multiphasic CT]. *Giornale Italiano di Radiologia Medica*. 2014;1:961-7.
 40. Bird JR, Brahm GL, Fung C, Sebastian S, Kirkpatrick IDC. Recommendations for the management of incidental hepatobiliary findings in adults: Endorsement and adaptation of the 2017 and 2013 ACR incidental findings committee white papers by the Canadian association of radiologists incidental findings working group. *Canada Assoc Rad J*. 2020;71(4):437-47.